

P_I-28

STEM-EELSによる構造および電子状態の解析

Structures and electron energy states analysis by STEM-EELS

越野 雅至¹, Tizei Luiz, H. G¹, Warner Jamie, H.², Cretu Ovidiu¹, 劉 崢¹, Lin Yung-Chang¹, Kuang He², 飯泉 陽子¹, 岡崎 俊也¹, 末永 和知¹

(¹産業技術総合研究所, ²オックスフォード大学)

Masanori Koshino¹, Luiz, H. G Tizei¹, Jamie, H. Warner², Ovidiu Cretu¹, Zheng Liu¹, Yung-Chang Lin¹, He Kuang², Yoko Iizumi¹, Toshiya Okazaki¹, Kazutomo Suenaga¹

(¹AIST, ²Department of Materials, University of Oxford)

P_I-29

二段シリンドリカルレンズを使用した新型モノクロメータ

A Novel Monochromater of Double Cylindrical Lenses

小川 貴志¹, 趙 福来¹

(¹韓国標準科学研究院)

Takashi Ogawa¹, Boklae Cho¹

(¹Korea Research Institute of Standards and Science)

P_I-30

ブラウンミレライト型構造Ca₂FeMnO₅における局所電子構造の研究

Local Electronic Structure Analysis of Ca₂FeMnO₅

治田 充貴¹, 保坂 祥輝¹, 市川 能也¹, 斉藤 貴志¹, 島川 祐一¹, 倉田 博基¹

(¹京都大学 化学研究所)

Mitsutaka Haruta¹, Yoshiteru Hosaka¹, Noriya Ichikawa¹, Takashi Saito¹, Yuichi Shimakawa¹, Hiroki Kurata¹

(¹Kyoto University)

P_I-31

EELSによるp (n)-a-Si/i-a-Si/c-Si多層膜におけるSiのディスオーダーの評価

Estimation of Si disorder in p (n)-a-Si/i-a-Si/c-Si heterojunctions by using EELS

東嶺 孝一^{1,2}, 及川 貴史¹, 小山 晃一^{1,2}, 大平 圭介^{1,2}, 松村 英樹^{1,2}

(¹北陸先端科学技術大学院大学, ²JST-CREST)

Koichi Higashimine^{1,2}, Takafumi Oikawa¹, Koichi Koyama^{1,2}, Keisuke Ohdaira^{1,2}, Hideki Matsumura^{1,2}

(¹Japan Advanced Institute of Science and Technology, ²JST-CREST)

P_I-32

Dual SDDを用いた半導体内ドーパント濃度の検出限界

Detection Limit of Dopant Concentration in Semiconductor using Dual SDD

福永 啓一¹, 遠藤 徳明¹, 鈴木 実², 近藤 行人¹

(¹日本電子株式会社, ²サーモサフィッシャーサイエントフィック株式会社)

Keiichi Fukunaga¹, Noriaki Endo¹, Minoru Suzuki², Yukihito Kondo¹

(¹JEOL Ltd., ²Thermo Fisher Scientific Japan)

P_I-33

孔無し位相板のクライオTEM観察への応用

Cryo TEM application with a hole-free phase plate

細木 直樹¹, 飯島 寛文¹

(¹日本電子株式会社)

Naoki Hosogi¹, Hirohumi Iijima¹

(¹JEOL Ltd.)

P_I-34

TEMを用いた高分子材料の液中観察方法の検討

A study of observation method of polymer materials in liquid using TEM

仲野 靖孝¹, 和山 真里奈¹, 渡邊 俊哉¹, 小川 太郎¹, 許斐 麻美¹, Pin Chang², Lin-Ai Tai², Yu-Ching Chen²

(¹株式会社 日立ハイテクノロジーズ, ²Bio Materials Analysis Technology, Incorporated)

Kiyotaka Nakano¹, Marina Wayama¹, Syunya Watanabe¹, Taro Ogawa¹, Mami Konomi¹, Chang Pin², Tai Lin-Ai², Chen Yu-Ching²

(¹Hitachi High-Technologies Corporation, ²Bio Materials Analysis Technology, Incorporated)

P_I-35

FE-ETEMを用いたガス雰囲気下における電極触媒の*in situ*観察

In situ observation of electrocatalysts in various gasses using FE-ETEM

白井 学¹, 松本 弘昭¹, 長沖 功¹, 矢口 紀恵¹

(¹(株)日立ハイテクノロジーズ)

Manabu Shirai¹, Hiroaki Matsumoto¹, Isao Nagaoki¹, Toshie Yaguchi¹

(¹Hitachi High-Technologies Corporation)

STEM-EELSによる低次元材料の構造および電子状態の解析

Structures and electron energy states analysis of low dimensional materials by STEM-EELS

越野 雅至¹, Tizei Luiz, H. G¹, Cretu Ovidiu¹, 劉 崢¹, Lin Yung-Chang¹, 飯泉 陽子¹, 岡崎 俊也¹, 末永 和知¹,

¹ National Institute of Advanced Industrial Science and Technology (AIST) Central 5, Tsukuba, Ibaraki 305-8565, JAPAN

Warner Jamie, H.², Kuang He²,

² Department of Materials, University of Oxford, United Kingdom

Abstract

We have demonstrated

1. molecule-by-molecule spectroscopy of individual fullerenes [1],
 2. atom-by-atom spectroscopy of graphene edges [2],
 3. atom-by-atom spectroscopy of N-doped graphene [3],
 4. atom-by-atom spectroscopy of tetra-vacancy in h-BN [4],
- by means of electron energy-loss spectroscopy (EELS) based on aberration-corrected scanning transmission electron microscopy (STEM).

Methods

Specimen preparations

Fullerene: Encapsulation inside a carbon nanotubes,
Sandwich between two monolayered h-BN sheets,
Graphene: CVD, PMMA-coat, transferred to SiN TEM grid,
Hexagonal-BN: CVD on Cu, polycarbonate-coat, HCl,

Instruments

S/TEM: JEM-2100F (30–60 kV)

Electron gun: Cold FEG (W111), FWHM = 0.35 eV,

Probe size = 0.1 nm,

Current 6–20 pA,

Delta-type aberration corrector (JEOL)

EELS: Gatan Quantum 965 for low voltage,

65 counts / electron,

50 μ s / sec for EELS,

Holder: A single tilt JEOL (Heating) holder

Data Processing:

Gatan Digital Micrograph 2,

HREM plugin (MSA, DeconvEELS),

ImageJ, Cornell Spectrum Imager (CSI) plugin,

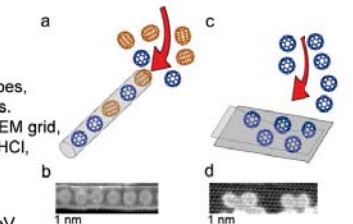


Figure 1-1: Fullerene storages: a-b) Model and ADF (Annular Dark Field) image of C60 (blue) and C70 (orange) molecules stored inside a SWNT. c-d) Model and ADF image of C60 (blue) molecules stored in between two layers of BN. The ADF image was taken at 30 kV for (b) and 60 kV for (d).



Figure 1-3: EELS simulation of C70 molecules: a) Depiction of a C70 molecule in two different orientations. Five non-identical carbon atoms are painted in different colors (b). Simulator of ELNES for different carbon atoms. Between the 285.7 eV and 287.7 eV peaks, the additional peak shifts for different atoms. This could explain the shifting peaks for the experimentally measured molecules. Note that C60 has 60 identical carbon atoms and will show no spectral variation due to the atoms involved in a spectrum.

Results & Discussion

1. Molecule-by-molecule spectroscopy of individual fullerenes [1].

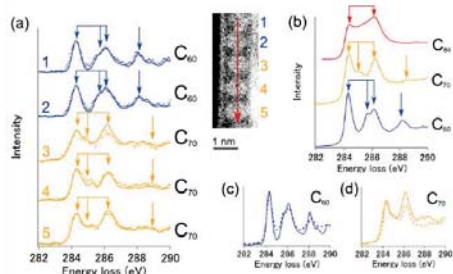


Figure 1-2: Core-level spectroscopy of individual fullerene molecules. a) ELNES carbon K edge spectra extracted from aligned five molecules shown in the inset on the right. Note that the contribution of carbon nanotube to the carbon K edge spectra has been extracted by recording separately the carbon K edge of an empty nanotube. The solid lines are spectra after Richardson-Lucy deconvolution and the dots are the raw data after background subtraction. Blue and orange arrows point to common features of C60 and C70, respectively (see text). From these spectra peak configurations, the discrimination of C60 and C70 molecules is indeed possible. (c) The same common features can be seen in (b) where reference spectra from crystalline C60, C70 and C84 are shown. The C84 spectra was extracted from Kuzuo et al [5] and obtained at 60 kV, while the others were obtained at 30 kV, as in the other experiments described here. Reference spectra for C60 and C70 crystals have been deconvoluted using the maximum entropy method. (c-d) Comparisons of the bulk crystalline spectrum (dashed-lines) with a single molecule spectrum (solid-lines) for C60 (blue) and C70 (orange), respectively. [5] R. Kuzuo, M. Terachi, M. Tanaka, Y. Saito, & H. Shinohara, Phys. Rev. B 49, 5054 (1994).

3. Atom-by-atom spectroscopy of N-doped graphene [3],

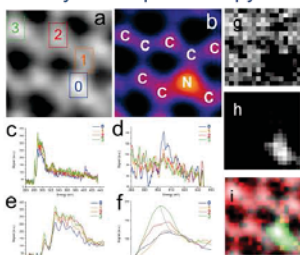


Figure 3-1: (a) ADF-STEM image taken simultaneously as the EELS map. (b) ADF-STEM image with high signal to noise of the same N dopant in graphene. (c-f) EELS corresponding to the boxed regions indicated in (a). (d-f) Magnified N K-edge, C K-edge, and π^* region of the C K-edge EELS corresponding to the boxed regions in (a). (g) 2D spectroscopic map based on the carbon K-edge EELS. (h) 2D spectroscopic map based on the N K-edge EELS signal. (i) Overlap of carbon EELS map (red) and N EELS map (green) with ADF-STEM image.

Figure 3-2: Density functional theory simulations of the EELS. Comparison of the experimental (a) and EELS of the C K-edge for nearest neighbour C atoms bonded to the N atom and C located several atoms away from the N atom and not bonded to it. (b) Comparison of the DFT EELS of the C K-edge for nearest neighbour C atom bonded to the N atom in N-doped graphene (blue line and modelled in c) and that in graphene (red line and modelled in d). Dashed vertical lines with labels (i)-(iii) indicate peaks for (i) π^* , (ii) σ^* , and (iii) peak for N bonded C atoms. (c) The N-doped graphene model has Amm2 symmetry with nitrogen atoms colored in red and carbon atoms with a core-hole colored in blue. (d) The graphene model has P-6mm symmetry with carbon atom with a core-hole colored in blue.

Results & Discussion

2. Atom-by-atom spectroscopy of graphene edges [2],

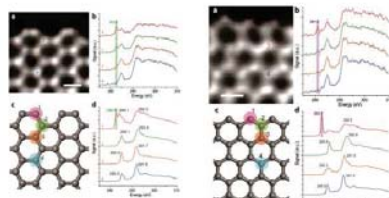


Figure 2-1: STEM-EELS mapping of an armchair graphene edge. (a) ADF-STEM image of armchair edge. Scale bar: 2 Å. (b) EELS from the numbered regions in (a). (c) Density functional theory atomic model of armchair edge. (d) Simulated EELS from the numbered regions in (c).

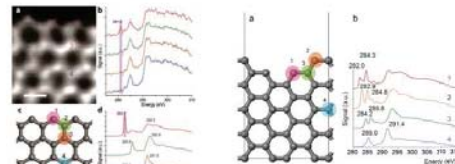


Figure 2-2: STEM-EELS mapping of a zig-zag graphene edge. (a) ADF-STEM image of zig-zag edge. Scale bar: 2 Å. (b) EELS from the numbered regions in (a). (c) Density functional theory atomic model of zig-zag edge. (d) Simulated EELS from the numbered regions in (c).

Figure 2-3: Model of stair edge (combination of armchair and zigzag edge) and ELNES simulation. Carbon K-edges of individual atoms numbered from 1 to 4 and marked by red, orange, green and blue colours in (a) are simulated in (b). The ELNES shape of stair edge is different from zigzag edge or armchair edge.

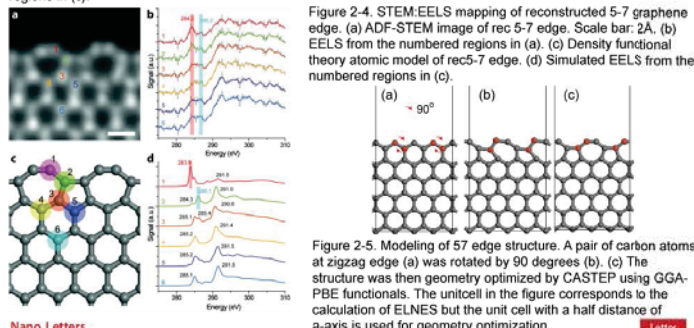


Figure 2-4: STEM-EELS mapping of reconstructed 5-7 graphene edge. (a) ADF-STEM image of rec 5-7 edge. Scale bar: 2 Å. (b) EELS from the numbered regions in (a). (c) Density functional theory atomic model of rec 5-7 edge. (d) Simulated EELS from the numbered regions in (c).

Nano Letters

Letter

Table 1. Summary of EELS Peak Positions for Different Graphene Edges

peak (eV)	zig-zag (P_1)	Klein (P_2)	armchair (P_3)	heptagon (P_4)	bulk (P_5)	pentagon (P_6)
experiment	281.0	282.8	284.2	284.2	285.0	286.2
DFT	282.7	283.5	284.6	283.9	285.0	286.1
shift (exp.)	-4.0	-2.2	-2.2	-0.8	0	+1.2
shift (DFT)	-2.3	-1.5	-2.4	-1.1	0	+1.1

4. Atom-by-atom spectroscopy of B-terminated tetra-vacancy in h-BN [4],

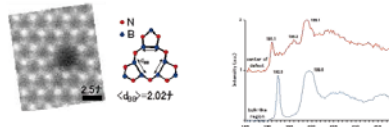


FIG. 4-1: High resolution ADF image of a VB1N3 tetra-vacancy in h-BN (left) and corresponding atomic model of the defect (right). Data acquired using 60 kV electrons @ 500 °C.

TABLE 1. h-BN defect types as a function of imaging conditions. The data in the shaded cells is taken from the literature.

Mode	Temperature	80 kV	60 kV
TEM	20 °C	VB1N3	VB1N3
STEM	500 °C	VB1N3	VB1N3

FIG. 4-2: The B K-edge EELS signature of a tetra-vacancy. The two spectra are acquired from the center of the defect and near the defect, respectively. The spectra have been PCA-filtered. The data was extracted from a 16x14 pixel map acquired using 60 kV electrons @ 600 °C, with an exposure time of 0.5 s/pix and an energy dispersion of 0.1 eV/ch.

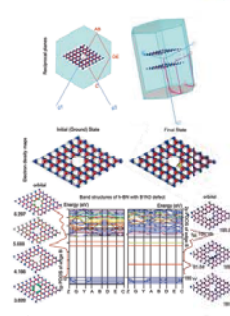


FIG. 4-3: Electron density maps, band structures for the ground and excited states electron configurations and partial density of states (PDOS) of 2p of the B atoms at the edge of the VB1N3 defect. The spatial distributions for bands (orbitals) corresponding to representative peaks in the PDOS are plotted for each case. See main text for details.

FIG. 4-4: (Left) ADF images of defects created in h-BN under 80 kV electron irradiation. The images have been FFT-filtered. At room temperature (upper row), B vacancies and VB1N3 defects dominate, while at high temperatures (lower row), N vacancies and VB1N3 defects are predominant. (Right) Distribution of the various types of defects created at 80 kV as a function of temperature. The error bars have been introduced in order to account for inaccuracies in structure assignment.

Summary

References

- [1] Luiz, H. G. Tizei, Zheng Liu, Masanori Koshino, Yoko Izumi, Toshiya Okazaki, and Kazu Suenaga. Single Molecular Spectroscopy: Identification of Individual Fullerene Molecules. Phys. Rev. Lett. 113, 185502-185502, Oct. 2014.
- [2] Warner, J. H.; Lin, Y.-C.; He, K.; Koshino, M.; Suenaga, K. Nano Lett., 14, 6155, Oct. 2014.
- [3] J. H. Warner, Y.-C. Lin, K. He, M. Koshino, K. Suenaga, Stability and Spectroscopy of Single Nitrogen Dopants in Graphene at Elevated Temperatures. ACS Nano, 8, 11806-11815, Dec. 2014.
- [4] O. Cretu, Y.-C. Lin, M. Koshino, L. H. G. Tizei, Z. Liu, K. Suenaga. Structure and Local Chemical Properties of Boron-Terminated Tetra-vacancies in Hexagonal Boron Nitride. Physical Review Letters, 114(7), 075502-075502, Feb 2015.

Acknowledgement

This work is partially supported by the JST Research Acceleration Programme.

Financial support by MEXT KAKENHI Grant No. 25107003 is acknowledged by Z. L.

Financial support by JSPS KAKENHI Grant No. 23681026 and No. 26390004 is acknowledged by M. K.



日本顕微鏡学会第71回学術講演会

優秀ポスター賞

[装 置 部 門]

STEM-EELSによる構造および電子状態の解析

越野 雅至¹, Tizei Luiz, H. G¹, Warner Jamie, H.²,
Cretu Ovidiu¹, 劉 崢¹, Lin Yung-Chang¹, Kuang He²,
飯泉 陽子¹, 岡崎 俊也¹, 末永 和知¹

¹産業技術総合研究所
²オックスフォード大学

平成27年5月13日～15日
日本顕微鏡学会第71回学術講演会
実行委員長 倉田 博基

